

Fatigue resistance curves for single and double shear riveted joints from old portuguese metallic bridges

Pedrosa, Bruno; Correia, José A.F.O.; Rebelo, Carlos; Lesiuk, Grzegorz; De Jesus, Abílio M.P.; Fernandes, António A.; Duda, M.; Calçada, Rui; Veljkovic, Milan

DOI

[10.1016/j.engfailanal.2018.10.009](https://doi.org/10.1016/j.engfailanal.2018.10.009)

Publication date

2019

Document Version

Final published version

Published in

Engineering Failure Analysis

Citation (APA)

Pedrosa, B., Correia, J. A. F. O., Rebelo, C., Lesiuk, G., De Jesus, A. M. P., Fernandes, A. A., Duda, M., Calçada, R., & Veljkovic, M. (2019). Fatigue resistance curves for single and double shear riveted joints from old portuguese metallic bridges. *Engineering Failure Analysis*, *96*, 255-273. <https://doi.org/10.1016/j.engfailanal.2018.10.009>

Important note

To cite this publication, please use the final published version (if applicable). Please check the document version above.

Copyright

Other than for strictly personal use, it is not permitted to download, forward or distribute the text or part of it, without the consent of the author(s) and/or copyright holder(s), unless the work is under an open content license such as Creative Commons.

Takedown policy

Please contact us and provide details if you believe this document breaches copyrights. We will remove access to the work immediately and investigate your claim.

Green Open Access added to TU Delft Institutional Repository

'You share, we take care!' – Taverne project

<https://www.openaccess.nl/en/you-share-we-take-care>

Otherwise as indicated in the copyright section: the publisher is the copyright holder of this work and the author uses the Dutch legislation to make this work public.



Fatigue resistance curves for single and double shear riveted joints from old portuguese metallic bridges



Bruno Pedrosa^{a,*}, José A.F.O. Correia^b, Carlos Rebelo^a, Grzegorz Lesiuk^c,
Abílio M.P. De Jesus^b, António A. Fernandes^b, M. Duda^c, Rui Calçada^b,
Milan Veljkovic^d

^a ISISE, Department of Civil Engineering, University of Coimbra, Rua Luís Reis Santos, Pólo II, 3030-788 Coimbra, Portugal.

^b Faculty of Engineering, University of Porto, Rua Dr. Roberto Frias, 4200-465 Porto, Portugal

^c Wrocław University of Science and Technology, Faculty of Mechanical Engineering, Department of Mechanics, Materials Science and Engineering, Smoluchowskiego 25, 50-370 Wrocław, Poland

^d Faculty of Civil Engineering and Geosciences, Delft University of Technology, Delft, Netherlands

ARTICLE INFO

Keywords:

Old riveted bridges
Fatigue behaviour of riveted joints
Statistical approach
Design recommendations

ABSTRACT

The maintenance and safety of ancient bridges is a major concern of governmental authorities. In particular, the safety of old riveted bridges fabricated and placed into service at the end of the 19th century deserves particular attention. These structures are susceptible to exhibit high fatigue damage levels due to their long operational period with increasing traffic intensity associated to an original design not covering the fatigue phenomenon. This paper reviews recent fatigue behaviour investigations on single and double shear riveted joints performed by Universities of Porto (Portugal), Trás-os-Montes e Alto Douro (Portugal), and Wrocław (Poland), in particular concerning the fatigue characterization of riveted joints extracted from representative Portuguese riveted bridges, namely the Eiffel, Luiz I, Fão, Pinhão and Trezói bridges. In order to overcome the influence of scatter and establish a reliable assessment for the obtained experimental data, two statistical approaches were used: implement linearized boundaries following the recommendation in ASTM E739 standard and defining probabilistic S–N fields using the Castillo & Fernández-Canteli model. This statistical analysis allows to propose design S–N curves for single and double riveted joints and evaluate the applicability (safety) of using the design curves suggested in Eurocode 3 as well as design curves proposed by Taras and Greiner.

1. Introduction

All over the world, a significant number of important infrastructures reached such a long service life with their structural safety had become a major concern for the governmental agencies. Metallic riveted road and railway bridges build in the end of the 19th and beginning of the 20th century are examples of civil engineering structures which are now subjected to completely different traffic conditions from those that were taken into account when they were designed. Fatigue assessment of these old riveted structures is now a concern not only because at that time designers were not fully aware of this phenomenon, but also because recent studies have shown that steel elements are prone to deteriorate under variable stresses [1–3].

Construction materials commonly used at the turn of 19th century were two types of steel –puddled and mild one. Technical

* Corresponding author.

E-mail address: bruno.pedrosa@uc.pt (B. Pedrosa).

<https://doi.org/10.1016/j.engfailanal.2018.10.009>

Received 4 June 2018; Received in revised form 18 September 2018; Accepted 17 October 2018

Available online 24 October 2018

1350-6307/ © 2018 Elsevier Ltd. All rights reserved.

Table 1
Chemical composition of puddle iron and mild low-carbon steel.

Material	C [%]	Mn [%]	Si [%]	P [%]	S [%]	N [ppm]
Puddle iron	Max. 0.08	0.4	n/a	0.6	0.04	n/a
Mild low-carbon steel	0.02–0.15	0.2–0.5	variable	0.03–0.06	0.02–0.15	variable
“Pomorski” bridge	0.02	0.05	0.03	0.24	0.048	n/a
Segment I (1885)						
“Pomorski” bridge	0.10	0.46	0.03	0.028	0.05	n/a
Segment II (1930)						
“Pomorski” bridge	0.170	0.52	0.03	0.05	0.05	n/a
Segment III (1930)						

infrastructures such as bridges made of those steel types and subjected to long operation periods show inclination towards degradation processes of their mechanical properties and chemical composition, which is well documented in previous authors' investigations [4–7]. The chemical composition and basic mechanical properties for puddle (called puddle iron) and mild steels are shown in Tables 1 and 2, respectively. For the old Portuguese metallic bridges built with old materials – puddle irons and medium steels – their monotonic mechanical properties, chemical composition, microstructures, as well as, fatigue properties can be found in refs. [8,9].

The brittle nature of such materials is strongly associated with its significant amount of slags and impurities as well as the susceptibility for microstructural degradation processes, mainly in steels with < 0.1%C content and with low content of Si. In general, these inclusions lead to an increase in the hardness and strength of the material, and to a decrease in the ductility, impact strength and crack resistance.

Therefore, structural changes in the material properties can be found, namely with the decomposition of pearlite or bainite areas into ferrite and carbides, as well as separation processes (nitrides and carbides).

Raposo et al. [10], Jesus et al. [11] and Correia et al. [12] identified in their investigations on steels and/or irons from old metallic bridges similar mechanical properties, microstructure and chemical composition to those identified by Lesiuk [4] in other materials from metallic bridges built in the same period.

Results reported by the authors demonstrate that these materials can be characterized as puddle iron and/or mild low-carbon steel, depending on the year of construction of each old metallic bridges. Student et al. [13] also studied microstructures and degradation mechanical characteristics of long term operated mild steel that was collected from Shukhov's tower. In this study, the authors suggested that the degradation of the steel properties has been caused by the development of scattering damages during their operation.

The “Pomorski” bridge is located in Wroclaw (Poland) and is composed of three parts (segments) erected in 1885 (segment I, puddle iron) and 1930 (segments II and III, mild steel). A microscopic view of the puddle and early mild steel which composed this structure is shown in Figs. 1 to 4.

Figs. 1 to 3 show the microscopic view for the segment I which correspond to puddle iron material while Figs. 4a) and 4b) correspond to the mild steel from segments II and III. In Fig. 1 can be observed a significant amount of discontinuities, non-metallic inclusions and delamination. In Fig. 2 is shown the ferrite grain structure with very high number of carbides and nitrides separations inside grains (A) and thick, continuous envelopes of Fe₃C at grain borders (B). Fig. 3 shows the ferrite grain interior decorated with separations not dissolved during heating and soaking for normalizing, which indicates for very advanced intensification of degrading processes. Furthermore, exemplary patterns (from segment II and III) of degraded structures can be seen in Fig. 4a) and 4b). The letter A in Fig. 4a) indicates ferrite grains with multiple cementite and nitrides separations, the letter B identifies thick envelope of Fe₃C and C point out partly degraded pearlite. In Fig. 4b) it is presented a microphotography of a sample from segment III (year 1930), which does not show any evidence of structural degrading. In Tables 1 and in Table 2 are also presented the chemical composition and mechanical properties for materials (Segment I, II and III) from the “Pomorski” bridge, respectively. For the Segment I, it can be observed some similarities to puddled irons, while segments II and III are from mild low-carbon steels family.

Fatigue phenomenon occur in areas where geometric discontinuities (or imperfections) origin high levels of stress concentration leading to the appearance of cracks [9,14]. This subject was initially investigated by Whöler and Spangenberg during the 19th

Table 2
– Mechanical properties of puddle iron and mild low-carbon steel.

Material	f_y [MPa]	f_u [MPa]	E [GPa]	A [%]	Z [%]
Puddle iron	220–280	330–400	170–200	< 25	n/a
Mild low-carbon steel	250–300	340–450	200–220	25–35	n/a
“Pomorski” bridge	239	361	190	18.9	n/a
First (1885)					
“Pomorski” bridge	298	423	205–210	35.0	n/a
Second (1930)					
“Pomorski” bridge	258	417	205–210	36.9	n/a
Third (1930)					

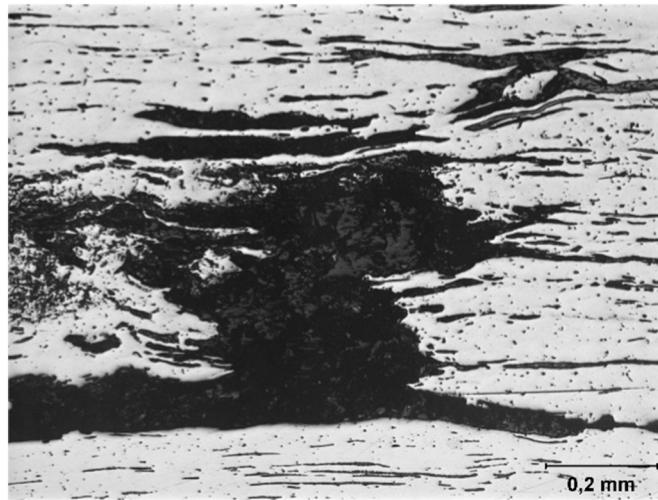


Fig. 1. - First Segment – the after-operating state (Sample 2-I, 1). Magnif. 100×, non-etched state [8].

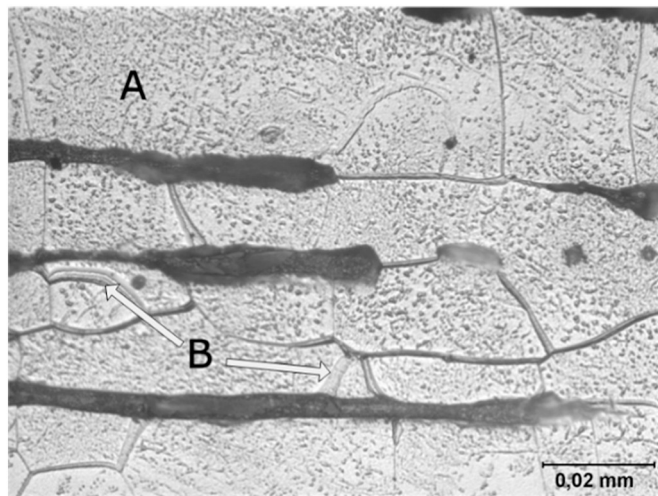


Fig. 2. - First Segment – after-operating state (Sample 2-I, 1). Magnif. 1000×, etched with 3% HNO_3 [8].

century. They were responsible for introducing fatigue S–N curves. Then, important contributes were made by Basquin, Coffin and Mason, Palmgreen and Miner, among others [15].

The evolution of the knowledge about the fatigue phenomenon lead to the appearance of new standards of design and construction, namely the part 1–9 of Eurocode 3 (EC3–1-9) [16]. This standard is based on a deterministic approach from experimental fatigue data of bolted and welded steel connections [17,18], which, as was previously stated, are not representative of old metallic riveted connections using puddled iron and mild low-carbon steel [18]. Although rivet joints are not explicitly referred in EC3 [16], experimental campaigns have shown that using detail category 71 seems to be a safe design criterion for riveted joints [19]. Taras and Greiner [20] have performed a statistical analysis of a significant amount of experimental fatigue data available in literature for riveted joints from old bridges. These authors suggested the categorization of the riveted joints into five categories. Two of the categories are the single and double shear splices under tensile loading. They also suggested the use of a slope, $m = 5$ for the design curve, instead of the $m = 3$ proposed EC3–1-9 [16].

In addition, Taras and Greiner [20] stated that mean stress effects must be accounted for riveted joints and suggested the use of a normalized stress range to allow the comparison of experimental fatigue data from distinct mean stresses which can be obtained as follows:

$$\Delta\sigma_{norm} = \frac{\Delta\sigma}{f(R_\sigma)} \quad (1)$$

where, $\Delta\sigma_{norm}$ is the normalized stress range, $\Delta\sigma$ is the tested stress range, $f(R_\sigma)$ is a normalization function to account for stress ratio effects, defined as a function of the material.

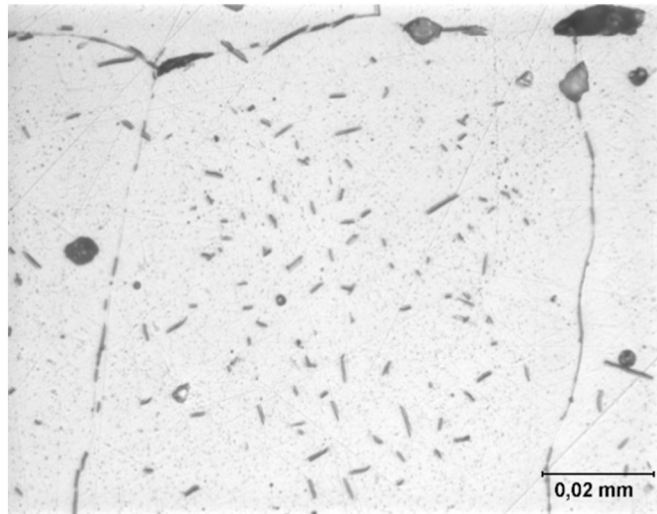


Fig. 3. - First segment – normalized state (Sample 2-1-6, 2). Magnif. 1000×, etched with 3% HNO_3 [8].

For wrought iron and mild steel manufactured before 1900, $f(R_\sigma)$ is defined as:

$$f(R_\sigma) = \frac{1 - R_\sigma}{1 - 0.7 \cdot R_\sigma} \leftarrow -1 \leq R_\sigma \leq 0 \quad f(R_\sigma) = \frac{1 - R_\sigma}{1 - 0.75 \cdot R_\sigma} \leftarrow R_\sigma > 0 \tag{2}$$

For mild steel after 1900 (St37, St48, St52, etc.) the following normalization function is proposed:

$$f(R_\sigma) = \frac{1 - R_\sigma}{1 - 0.4 \cdot R_\sigma} \leftarrow -1 \leq R_\sigma \leq 0 \quad f(R_\sigma) = \frac{1 - R_\sigma}{1 - 0.6 \cdot R_\sigma} \leftarrow R_\sigma > 0 \tag{3}$$

This paper intends to contribute for the state of knowledge concerning the fatigue behaviour of riveted joints made of old steel extracted from representative Portuguese bridges. The results of various experimental programs are presented, whose main objective was to characterize the fatigue resistance of riveted joints extracted from Eiffel, Luiz I, Pinhão and Trezói bridges, and riveted joints manufactured using original material from the Fão bridge.

A statistical analysis on this representative fatigue experimental data is performed following the recommendations in ASTM E739 [21] which is materialized by linearized statistical boundaries and implementing the Castillo & Fernández-Canteli model [22] for defining the probabilistic S–N fields [23,24]. The main goal of this statistical analysis is to propose alternative design S–N curves which can be representative for the fatigue experimental data of riveted joints and compare them with the recommendations prescribed in EC3–1-9 [16] and the design curve proposed by Taras and Greiner [20].

2. Statistical models for fatigue data

The influence of scatter on fatigue data has been studied. It is known that several sources of scatter may affect fatigue results on laboratory experiments, namely at the specimen production (surface quality) and/or during the tests (accuracy of test equipment) [25]. Therefore, using statistical approaches to fatigue problems is essential to establish reliable assessments. S–N curves can be computed taking into account the influence of scatter using statistical approaches. Experimental investigations have shown that the influence of scatter raises as the stress amplitude decreases – [26] – see Fig. 5. Schijve [26] studied the implementation of a statistical distribution function using $\log(N - N_0)$ -normal and the 3-parameter Weibull distribution. However, this investigation focused to describe specific location of S–N fields rather than the complete distribution.

More recently, researches have been performed aiming to overcome this problem and try to model the complete S–N field (see refs. [27–30]). Castillo and Fernández-Canteli [22] developed a probabilistic model supported by both physical and statistical assumptions. It is recommended for medium to high or even very high cycle fatigue regimes. Probabilistic S–N fields can be applied to describe the fatigue behaviour of mechanical details or structural components including the consideration of run-outs. A more detailed description of this model will be presented latter in this paper.

The standard practice in engineering is to perform a linear regression analysis on $\log(N_f)$ vs $\log(\Delta\sigma)$ data in order to compute the mean S–N curve and establish the safety margins by shifting it using the standard deviation of the residuals as shows Eq. (4):

$$Y = A + B \cdot X \pm \alpha \cdot S \tag{4}$$

where Y is the dependent variable defined as $\log(N_f)$, X is the independent variable defined as $\log(\Delta\sigma)$, N_f is the number of cycles to failure, $\Delta\sigma$ is the stress range, A and B are linear regression parameters which are related to the C and m constants:

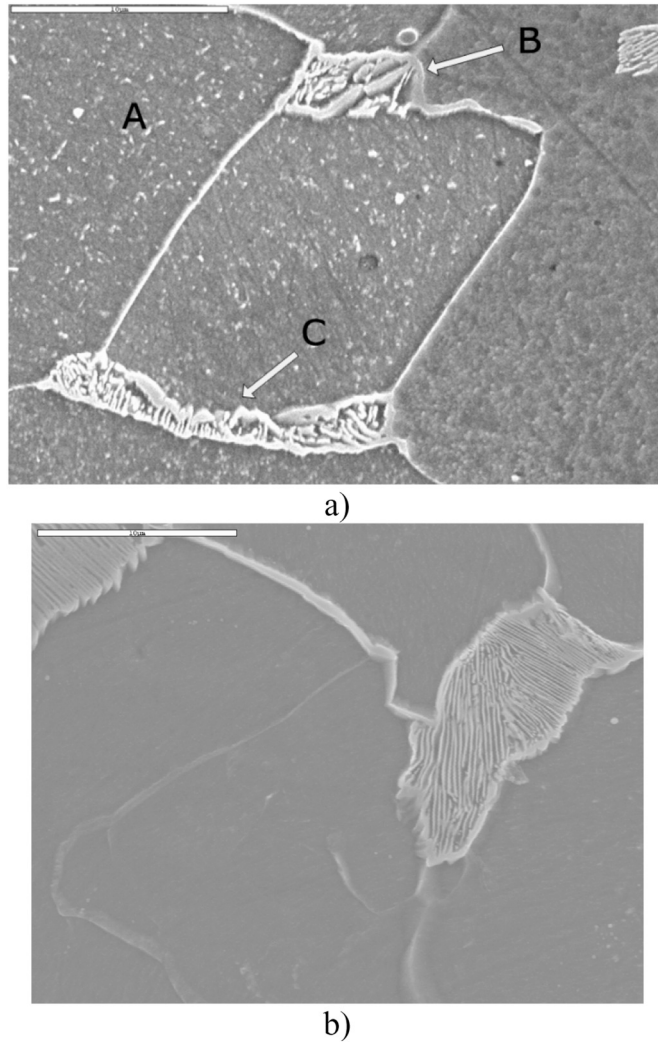


Fig. 4. a) - Sample from the segment II in the as-operated state, magnification 4300 × (SEM), etched with 3%HNO₃; b) - Sample from segment III in the as-operated state, magnification 4300 × (SEM), etched with 3%HNO₃ [8].

$$\begin{cases} C = 10^A \\ m = -B \end{cases} \tag{5}$$

For the estimation of *A* and *B* parameters, Eq. (6) and Eq. (7) should be used where \bar{Y} and \bar{X} are the mean values of the experimental data $X_i = \log \Delta\sigma_i$ and $Y_i = \log N_{f, i}$, respectively and *n* is the number of tested specimens.

$$A = \bar{Y} - B \cdot \bar{X} \tag{6}$$

$$B = \frac{\sum_{i=1}^n (X_i - \bar{X})(Y_i - \bar{Y})}{\sum_{i=1}^n (X_i - \bar{X})^2} \tag{7}$$

Rectilinear confident bands are implemented as shows Eq. (4), with α as an integer number (in this analysis it is assumed $\alpha = 1$ or 2) and *S* is the standard deviation of the residuals calculated from Eq. (8). If α assumes value 1, the confidence band will cover approximately 68% of the obtained data, whereas if α is equal to 2, the covered values will rise to around 95%.

$$S^2 = \frac{\sum_{i=1}^n (Y_i - A - B \cdot X_i)^2}{n - 2} \tag{8}$$

This is the approach stated in material standards such as the ASTM E739 standard [21]. In spite of being a common way to deal with fatigue problems, it does not produce reliable estimations for high cycle fatigue regimes as well as do not have in account the variable scatter along the fatigue domain. Its main advantage is its easy implementation.

The previously referred Castillo and Fernández-Canteli model [22] defines the probabilistic S–N field respecting the necessary

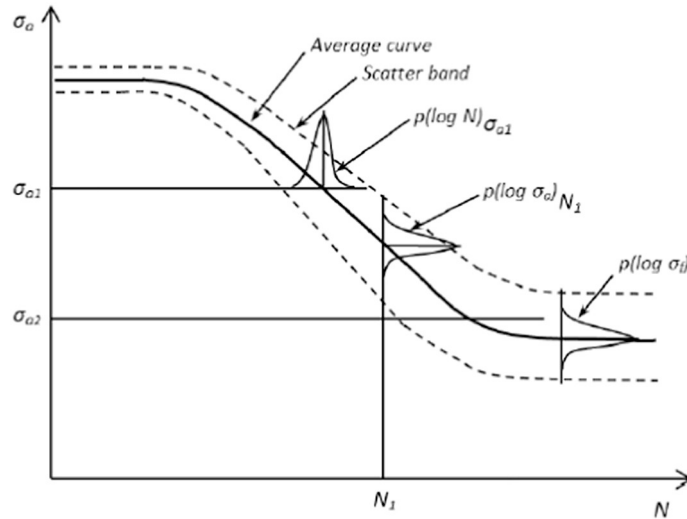


Fig. 5. – Typical distribution of scatter in a S–N curve [26].

compatibility between lifetime distribution for a given stress range and stress range distribution for a given lifetime using a functional equation:

$$F(\log N_f; \log \Delta\sigma) = p = 1 - \exp \left\{ - \left[\frac{(\log N_f - B)(\log \Delta\sigma - C) - \lambda}{\delta} \right]^\beta \right\} \tag{9}$$

where N_f is the number of cycles at failure; $\Delta\sigma$ is the stress level; $F()$ is the cumulative probability distribution function of N_f for a given $\Delta\sigma$, $B = \log(N_0)$, N_0 being a threshold value of lifetime; $C = \log(\Delta\sigma_0)$, $\Delta\sigma_0$ being the endurance fatigue limit; λ , β and δ are non-dimensional model parameters (β : Weibull shape parameter, δ : Weibull scale parameter and λ : Weibull location parameter defining the position of the zero-percentile curve).

Weibull probabilistic S–N fields (Fig. 6) are established between the lifetime thresholds defined by a horizontal asymptote ($\log N_f = B$) and a vertical asymptote ($\log \Delta\sigma = C$) for the most representative percentile curves (hyperbolas), $p = 0$, $p = 0.05$, $p = 0.5$, $p = 0.95$.

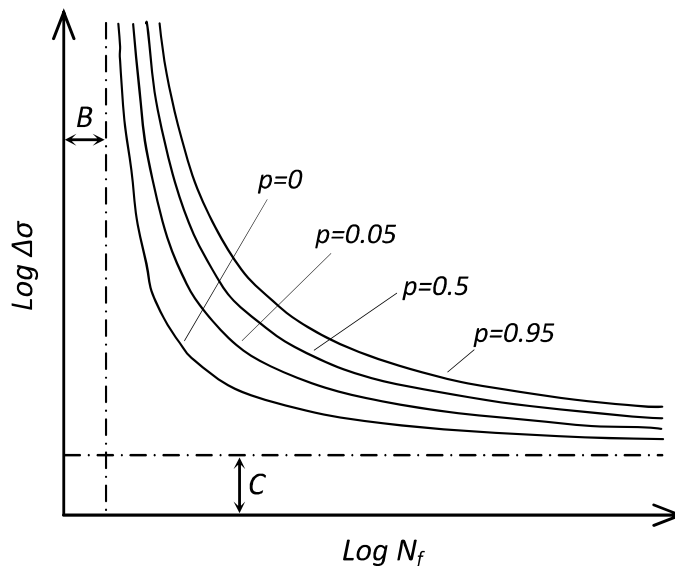


Fig. 6. - Probabilistic S–N field according to the Weibull model proposed by Castillo and Fernández-Canteli [15].

Table 3
- Results of the fatigue tests of the riveted joints from the Luiz I bridge [31].

Specimen	S_{gross}	S_{net}	R_{σ}	F_{max}	ΔF	f	$\Delta\sigma_{gross}$	$\Delta\sigma_{net}$	N_f
–	mm ²	mm ²	–	N	N	Hz	MPa	MPa	Cycles
S5R1	350.0	210.0	0.1	31,500	28,350	8.0	81.0	135.0	164,985
S5R2	350.0	210.0		31,500	28,350	6.0	81.0	135.0	426,259
S5R3	350.0	210.0		26,600	23,940	7.0	68.4	114.0	161,801
S5R4	350.0	210.0		22,600	20,340	7.0	58.1	96.9	999,453
S5R5	350.0	210.0		19,200	17,280	7.0	49.4	82.3	514,569
S5R6	350.0	210.0		16,330	14,697	8.0	42.0	70.0	1,586,560
S5R7	350.0	210.0		14,000	12,600	8.0	36.0	60.0	904,586

3. Fatigue experimental data of riveted connections

Fatigue experimental tests have been performed in order to evaluate the fatigue resistance of riveted joints made of original materials from Portuguese old bridges [31–35]. Riveted joints were extracted from Eiffel, Luiz I, Pinhão and Trezói bridges. In addition, riveted joints were manufactured using original material from the Fão bridge, but applying new rivets. This available S–N fatigue data from riveted connections intend to be representative of old metallic riveted Portuguese bridges. Experimental data is presented in the form of S–N or Wöhler curves, which shows a power relationship between the applied stress range ($\Delta\sigma$) and the corresponding number of cycles to failure (N_f).

All fatigue tests were performed on servo-hydraulic machines rated to 100kN or 250kN and subjected to load control conditions. The obtained results from the fatigue tests of single shear riveted connections extracted from Luiz I, Pinhão and Trezói bridges and from fatigue tests of double shear riveted connections extracted from Eiffel and Fão bridges are summarized, respectively in Table 3, Table 4, Table 5, Table 6 and Table 7, where S_{gross} is the gross cross-section, S_{net} is the net cross-section, R_{σ} is the stress ratio, F_{max} is the maximum testing force, ΔF is the test load range, f is the test frequency, $\Delta\sigma_{gross}$ is the stress range computed on the gross cross-section, $\Delta\sigma_{net}$ is the stress range calculated in the net cross-section and N_f is the number of cycles to failure [31–35]. The gross cross-section corresponds to the remote section of the joint, while the net cross-section corresponds to the section excluding the rivet hole.

Both statistical models presented in the previous chapter are implemented for the analysis of the obtained data: ASTM E739 [21] recommendations and the probabilistic model proposed by Castillo and Fernández-Canteli [22]. Afterwards, the reliability of using the recommended design curve proposed on EC3–1-9 [16] characterized by a stress amplitude, $\Delta\sigma$, of 71 MPa at 2 million cycles for the obtained data is assessed as well as the design criterion proposed by Taras and Greiner [20] defined by $\Delta\sigma_C = 71$ MPa and $m = 5$.

3.1. Single shear riveted connections

3.1.1. Luiz I bridge

Original single shear riveted specimens with one rivet extracted from Luiz I bridge whose geometry is illustrated in Fig. 7 were tested under fatigue loading conditions. Due to limitations imposed by the available material, only single lap joints were tested. A total of 7 specimens were tested under $R_{\sigma} = 0.1$ and test frequencies, f , ranged between 6 and 8 Hz. The obtained results are summarized in Table 3.

Fatigue results from riveted joint of Luiz I bridge were plotted on a S–N logarithmic scale as presented in Fig. 8. The statistical approach recommended on ASTM E 739–9 [21] and the probabilistic model proposed by Castillo and Fernández-Canteli [22] were implemented on the obtained fatigue data. The probabilistic S–N fields were defined together with the percentile curves corresponding to probabilities of failure of 5%, 50% and 95%.

Table 4
- Results of the fatigue tests for riveted joints from the Trezói bridge [33,34].

Specimen	S_{gross}	S_{net}	R_{σ}	F_{max}	ΔF	f	$\Delta\sigma_{gross}$	$\Delta\sigma_{net}$	N_f
–	mm ²	mm ²	–	N	N	Hz	MPa	MPa	cycles
F1	591.3	328.5	0.1	71,000	63,900	4.0	108.1	194.5	50,771
F2	580.5	322.5		47,500	42,750	6.0	73.6	132.6	605,387
F3	585.9	325.5		47,500	42,750	6.0	73.0	131.3	566,477
F4	495.8	235.4		30,000	27,000	10.0	54.5	114.7	2,518,224
F5	540.0	280.8		33,000	29,700	10.0	55.0	105.8	1,202,674
F6	498.1	236.5		36,200	32,580	8.0	65.4	137.8	846,982
F7	499.1	239.7		29,000	26,100	10.0	52.3	108.9	4,901,965
F8	540.0	280.8		33,000	29,700	10.0	55.0	105.8	3,473,620

Table 5
- Results of the fatigue tests of riveted joints from the **Pinhão bridge** [32].

Specimen	S_{gross}	S_{net}	R_{σ}	F_{max}	ΔF	f	$\Delta\sigma_{gross}$	$\Delta\sigma_{net}$	N_f
–	mm ²	mm ²	–	N	N	Hz	MPa	MPa	cycles
CF1	460.3	269.3	0.1	25,000	22,500	6.0	48.9	83.5	1,922,024
CF2	458.4	267.4		50,000	45,000	6.0	98.2	168.3	86,140
CF3	459.4	268.4		37,000	33,300	6.0	72.5	124.1	635,172
CF4	460.3	269.3		31,000	27,900	6.0	60.6	103.6	574,452
CF5	460.3	269.3		18,500	16,650	6.0	36.2	61.8	1,450,789
CF6	460.3	269.3		25,000	22,500	6.0	48.9	83.5	2,243,676
CF7	460.3	269.3		18,500	16,650	6.0	36.2	61.8	10,000,000→

Table 6
- Results of the fatigue tests of the riveted joints from the **Eiffel bridge** [35].

Specimen	S_{gross}	S_{net}	R_{σ}	F_{max}	ΔF	f	$\Delta\sigma_{gross}$	$\Delta\sigma_{net}$	N_f
–	mm ²	mm ²	–	N	N	Hz	MPa	MPa	cycles
V1	430.1	296.8	0.1	55,533	49,980	5.0	116.2	168.4	1,513,265
V2	427.3	293.5		54,939	49,445	7.5	115.7	168.4	1,500,331
V3	445.3	278.7		57,538	51,784	7.5	116.3	185.8	240,383
V4	432.0	299.6		55,640	50,076	7.5	115.9	167.1	149,378
V5	433.7	303.3		67,551	60,796	5.0	140.2	200.5	61,456
V6	442.2	301.2		69,239	62,315	5.0	140.9	206.9	149,879
V7	427.9	280.4		66,115	59,504	5.0	139.1	212.2	19,768
V8	437.8	308.1		68,511	61,660	5.0	140.8	200.2	12,195
V9	431.2	304.3		61,121	55,009	5.0	127.6	180.8	31,954
V10	438.1	306.9		62,122	55,910	5.0	127.6	182.1	53,638
V11	441.4	285.9		63,062	56,756	5.0	128.6	198.5	114,510
V12	452.8	311.2		64,352	57,917	5.0	127.9	186.1	23,196
V13	428.5	259.0		54,480	49,032	5.0	114.4	189.3	91,069
V14	431.1	309.3		66,909	60,218	5.0	139.7	194.7	12,950

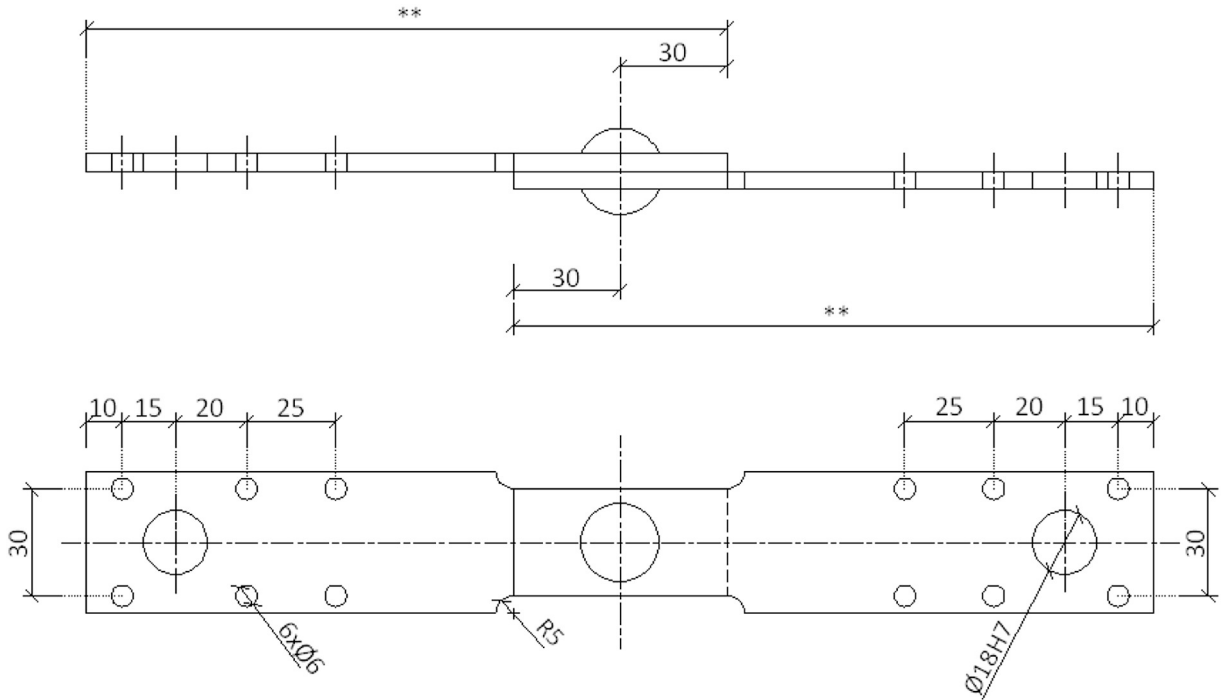
Table 7
- Results of the fatigue tests for riveted joints from the **Fão bridge** [35].

Specimen	S_{gross}	S_{net}	R_{σ}	F_{max}	ΔF	f	$\Delta\sigma_{gross}$	$\Delta\sigma_{net}$	N_f
–	mm ²	mm ²	–	N	N	Hz	MPa	MPa	cycles
FA1	342.2	160.2	0.01	56,940	56,370.6	2.5	164.7	351.9	9744
FA2	345.7	163.8		58,210	57,627.9	2.5	166.7	351.9	5285
FA3	342.9	162.3		57,690	57,113.1	2.5	166.5	351.9	24,357
FA4	340.9	160.3		56,960	56,390.4	5.0	165.4	351.9	3458
FA5	333.6	157.8		49,300	48,807	2.5	146.3	309.3	141,330
FA6	329.4	155.5		48,570	48,084.3	5.0	146.0	309.3	52,879
FA7	349.2	165.6		51,730	51,212.7	5.0	146.6	309.3	6644
FA8	345.6	163.8		51,160	50,648.4	5.0	146.5	309.2	21,050
FA9	344.3	163.1		47,430	46,955.7	5.0	136.4	287.9	38,242
FA10	344.0	163.4		47,530	47,054.7	5.0	136.8	287.9	103,809
FA11	345.9	163.1		47,430	46,955.7	5.0	135.8	287.9	75,749
FA12	343.7	163.0		35,120	34,768.8	5.0	101.2	213.3	210,995
FA13	327.7	155.3		26,770	26,502.3	5.0	80.9	170.7	699,161
FA14	347.2	160.8		27,700	27,423	10.0	79.0	170.6	4,000,000→
FA15	338.7	159.7		27,520	27,244.8	5.0	80.5	170.6	1,439,414

3.1.2. *Trezói bridge*

Riveted joints with a single rivet and one shear plane were machined from an original bracing member removed from the Trezói bridge. The final dimensions of the riveted joints are illustrated in Fig. 9. The original rivets of the connections were preserved. The riveted joints were tested under fatigue loading conditions with a stress R-ratio equal to 0.1 and test frequencies, f , ranging between 4 and 10 Hz. The S–N data is summarized in Table 4 [33,34]. Some failures were generated at cracks that initiated at the rivet hole and propagated through the net cross section; other failures were due to cracks initiated and propagated outside the net cross section, motivated by important clamping forces on the rivets. The true value of the clamping forces in the rivets is, in general, difficult to assess and in this case were not measured.

Fatigue results from riveted joint of Trezói bridge were also plotted on a S–N logarithmic scale as presented in Fig. 10. The



** Maximum dimension allowing equal dimension of side plates.

Fig. 7. - Nominal geometry of the riveted joint from the Luiz I bridge [31]

**Maximum dimension allowing equal dimension of side plates.

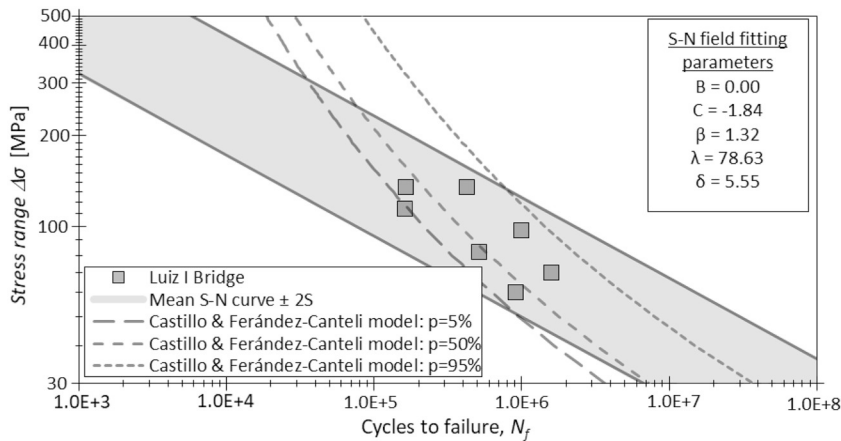


Fig. 8. - S–N fatigue data from riveted joint of Luiz I bridge: statistical analysis using linearized boundaries and Castillo & Fernández-Canteli model [22] (*p* corresponds to probability of failure).

statistical approach recommended on ASTM E 739–9 [21] and the probabilistic model proposed by Castillo and Fernández-Canteli [22] were implemented on the obtained fatigue data. The probabilistic S–N fields were defined together with the percentile curves corresponding to probabilities of failure of 5%, 50% and 95%.

3.1.3. Pinhão bridge

Fig. 11 illustrates the geometry of the original riveted specimens extracted from the Pinhão bridge, which was similar to the specimens extracted from the Luiz I bridge. An approximate thickness of the plates between 10 and 11 mm was measured for those specimens. The observation of a macrograph of the rivet longitudinal section allow us the estimation of the hole diameter (Ø21mm) and the rivet diameter (Ø20mm). A total of seven specimens were tested under load control, with stress R-ratio, $R\sigma = 0.1$. The number of specimens was limited by the amount of available material. The results of the fatigue tests are summarized in Table 5. The

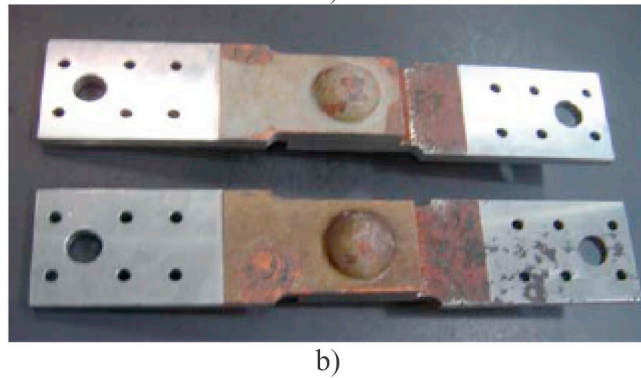
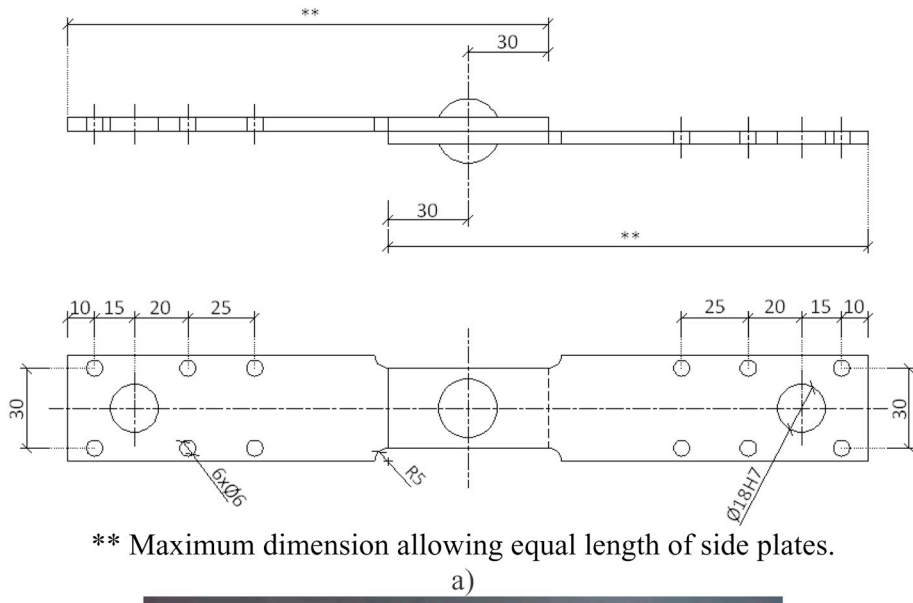


Fig. 9. - Riveted joint prepared with material from the Trezói bridge: a) geometry of the riveted joint (dimensions in mm); b) view of the riveted specimens [33,34].

**Maximum dimension allowing equal length of side plates.

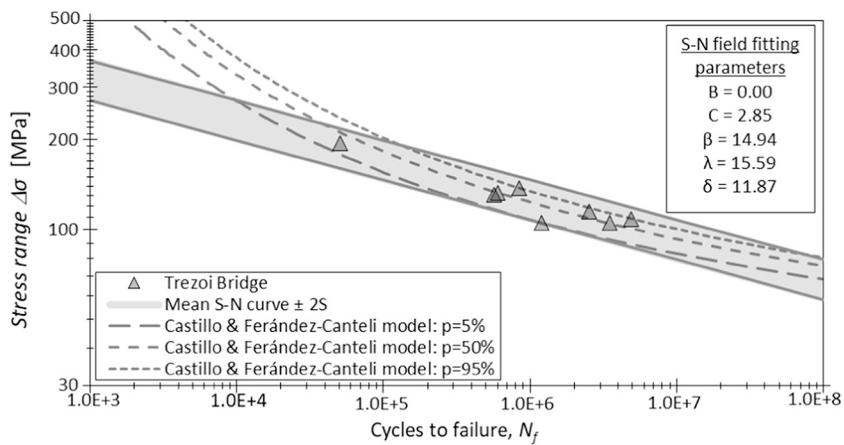
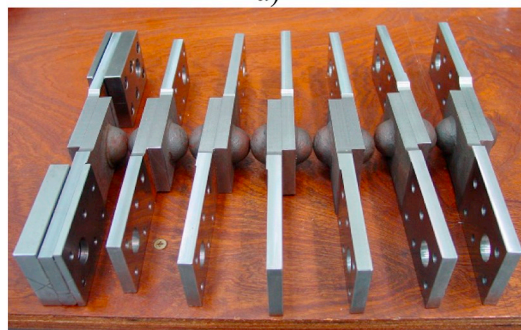
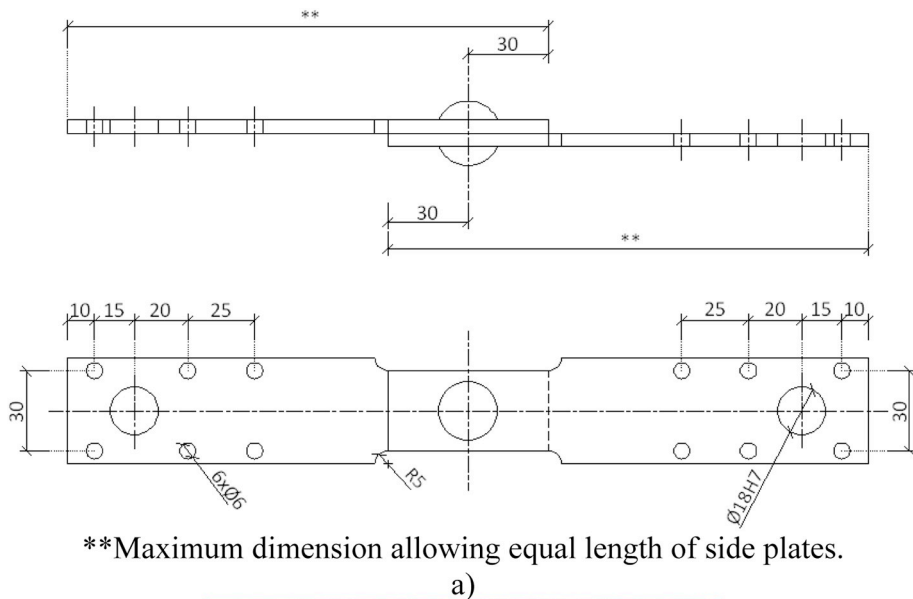


Fig. 10. - S–N fatigue data from riveted joint of Trezói bridge: statistical analysis using linearized boundaries and Castillo & Fernández-Canteli model [22] (p corresponds to probability of failure).



b)

Fig. 11. - Riveted joint specimens prepared with the material from the Pinhão bridge: a) geometry of the riveted joint (dimensions in mm); b) view of the riveted specimens [32].

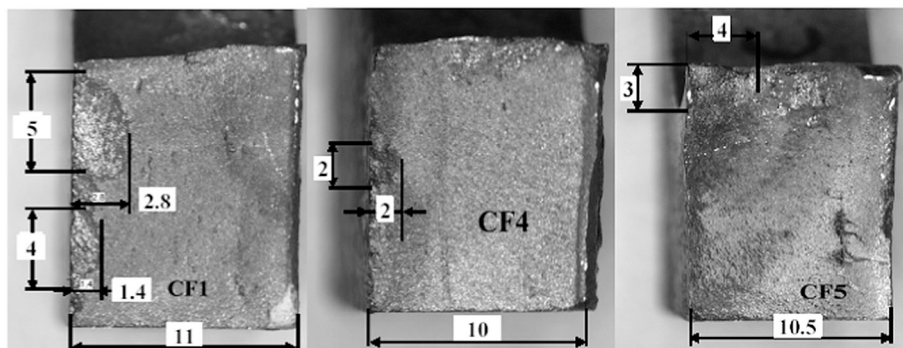


Fig. 12. - Initial crack-like flaws observed in some tested riveted specimens from the Pinhão bridge [32].

fracture surfaces of specimens CF1, CF4 and CF5 show that the fatigue cracks initiated at existing flaws as illustrated in Fig. 12.

**Maximum dimension allowing equal length of side plates.

Fatigue results from riveted joint of Trezói bridge were also plotted on a S–N logarithmic scale as presented in Fig. 13. The statistical approach recommended on ASTM E 739–9 [21] and the probabilistic model proposed by Castillo and Fernández-Canteli [22] were implemented on the obtained fatigue data. The probabilistic S–N fields were defined together with the percentile curves corresponding to probabilities of failure of 5%, 50% and 95%.

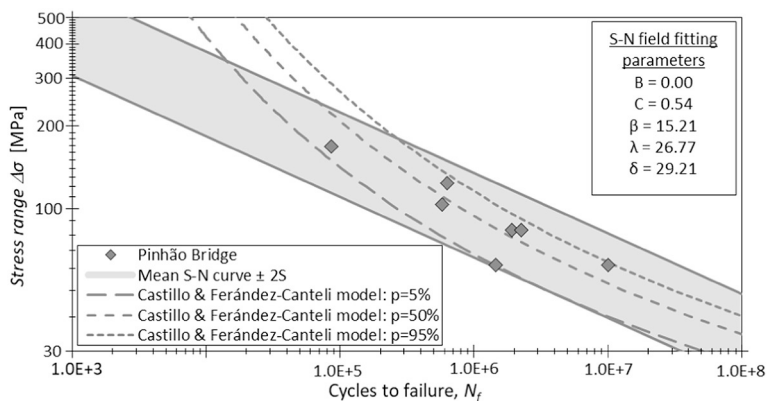


Fig. 13. - S–N fatigue data from riveted joint of **Pinhão bridge**: statistical analysis using linearized boundaries and Castillo & Fernández-Canteli model [22] (p corresponds to probability of failure).

3.2. Double shear riveted connections

3.2.1. Eiffel bridge

Double shear riveted connections were cut out from the web of a girder from the Darque south viaduct of the Eiffel bridge. Based

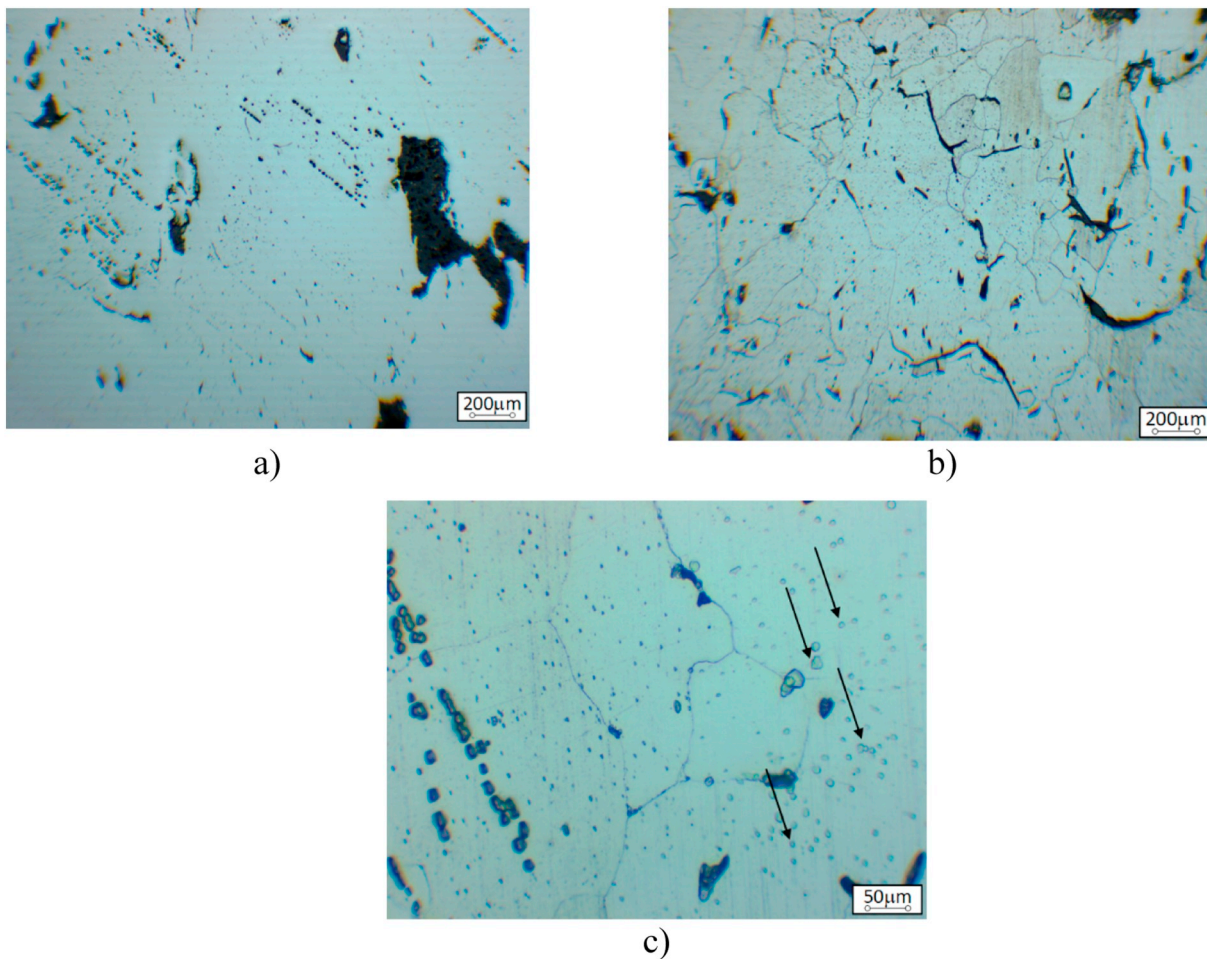


Fig. 14. – Microstructure of from riveted specimens extracted from the **Eiffel bridge**: a) large multiphase non-metallic inclusions, non-etched state; b) ferrite grains structure with non-metallic inclusions – typical for puddle iron different grain size, etched 5% HNO_3 ; c) enlarged microstructure with non-metallic inclusions chains, ferrite grains with microstructural degradation symptoms (marked by arrows), etched 5% HNO_3 .

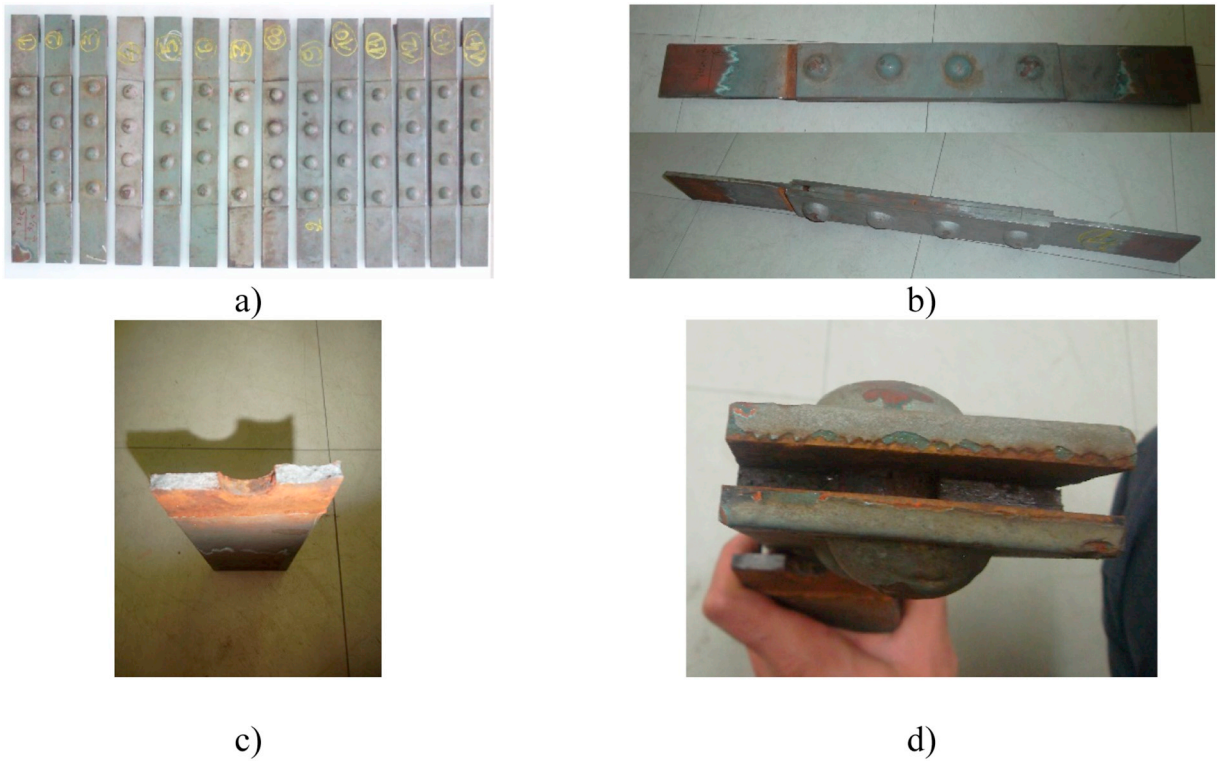


Fig. 15. - Riveted specimens extracted from the Eiffel bridge: a) complete test series; b), c) and d) illustration of the specimen, before and after fatigue failure [35].

on the microscopic view presented in Fig. 14, it should be noted that these materials belong to puddle iron material group with presence of large slags and impurities.

Specimens were cut along the longitudinal direction and the respective mid plates showed an average thickness of 6.7 mm. Fig. 15 illustrates the complete test series of the riveted specimens extracted from the Eiffel bridge. A total of 14 specimens were tested under a stress R-ratio equal to 0.1 and frequencies, f , ranged between 5 and 7.5 Hz. Each specimen exhibits a single row of four rivets, aligned in the loading direction. The results of these fatigue tests are summarized in Table 6.

Fatigue results from riveted joint of Trezói bridge were also plotted on a S–N logarithmic scale as presented in Fig. 16. The statistical approach recommended on ASTM E 739–9 [21] and the probabilistic model proposed by Castillo and Fernández-Canteli [22] were implemented on the obtained fatigue data. The probabilistic S–N fields were defined together with the percentile curves corresponding to probabilities of failure of 5%, 50% and 95%.

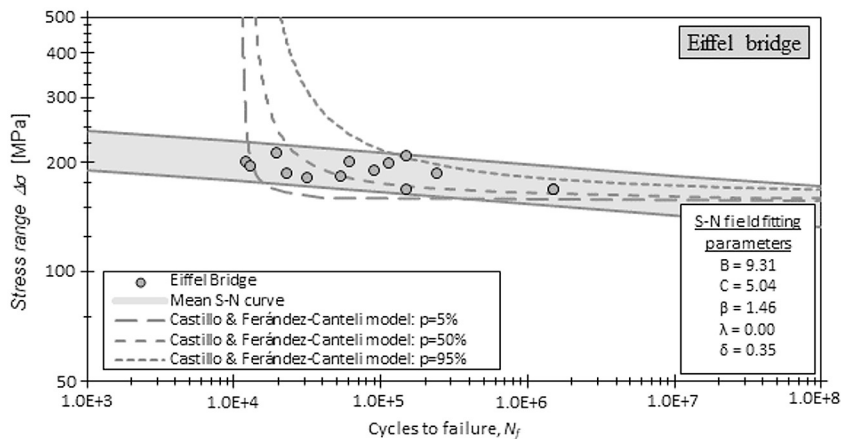


Fig. 16. - S–N fatigue data from riveted joint of Eiffel bridge: statistical analysis using linearized boundaries and Castillo & Fernández-Canteli model [22] (p corresponds to probability of failure).

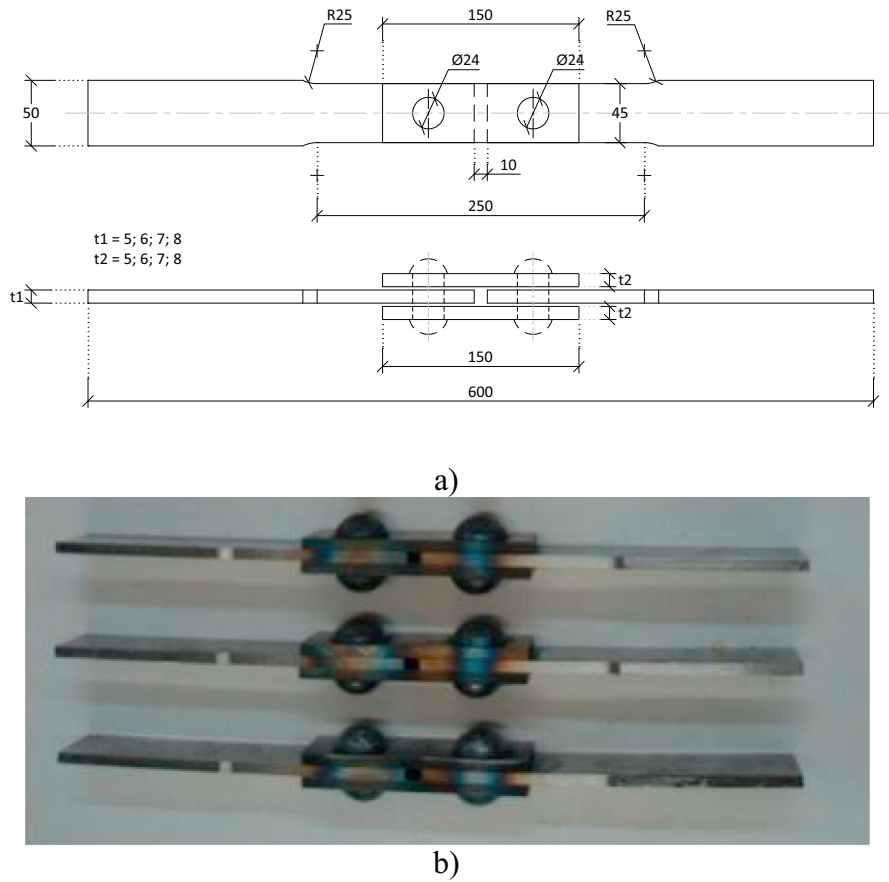


Fig. 17. – Riveted joint prepared with the material from the Fão bridge: a) geometry of the riveted joint (dimensions in mm); b) views of the riveted specimens [35].

3.2.2. Fão bridge

Specimens manufactured with the original material from the Fão bridge were also double shear connections, as shown in Fig. 17. In this case, only two rivets were applied and the plate thickness ranged between 5 and 8 mm. New holes were drilled with a diameter of 24 mm and rivets with a diameter of 22 mm were used to assemble the plates. The clearance between rivets and holes were filled due to the expansion of the rivets. A total of 15 specimens were tested under stress ratio $R_\sigma = 0.0$ and test frequencies, f , ranging between 2.5 and 12 Hz. Table 7 summarizes the results of the fatigue tests obtained for these riveted specimens.

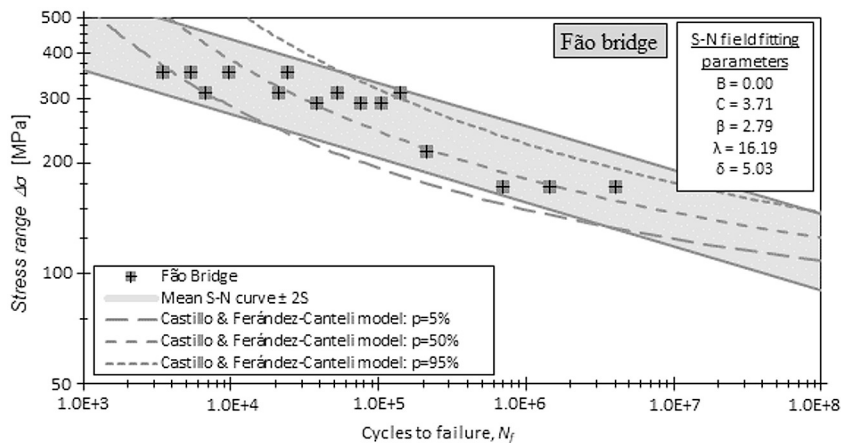


Fig. 18. - S–N fatigue data from riveted joint of Fão bridge: statistical analysis using linearized boundaries and Castillo & Fernández-Canteli model [22] (p corresponds to probability of failure).

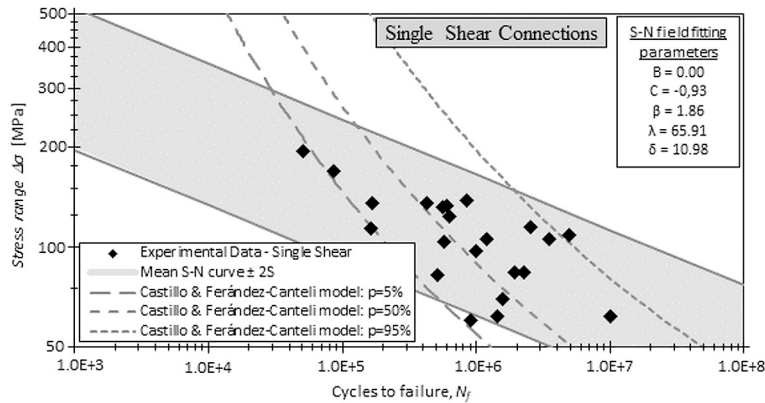


Fig. 19. - S–N fatigue data from **single shear riveted connections** from Portuguese old bridges: statistical analysis using linearized boundaries and Castillo & Fernández-Canteli model [22] (p corresponds to probability of failure).

Fatigue results from riveted joint of Trezói bridge were also plotted on a S–N logarithmic scale as presented in Fig. 18. The statistical approach recommended on ASTM E 739–9 [21] and the probabilistic model proposed by Castillo and Fernández-Canteli [22] were implemented on the obtained fatigue data. The probabilistic S–N fields were defined together with the percentile curves corresponding to probabilities of failure of 5%, 50% and 95%.

4. Results and discussion

All the fatigue data obtained from both single and double shear riveted connections were plotted in one graph as show Figs. 19 and 20, respectively. Both ASTM E379 [21] recommendations and Castillo and Fernández-Canteli model [22] were applied to the fatigue data. The rectilinear confident bands established in ASTM E379 [21] were defined by shifting the mean S–N curve with two times the standard deviation. The probabilistic S–N fields were defined together with the percentile curves corresponding to probabilities of failure of 5%, 50% and 95%.

Fig. 21 and Fig. 22 compare the S–N data from riveted joints of Portuguese bridges with S–N data from Taras and Greiner investigation [20], concerning single and double joints, respectively. Also EC3–1-9 [16] detail 71 is presented. For double shear riveted joints, Taras and Greiner [20] proposed a design S–N curve with a slope, $m = 5$ and a fatigue strength of 90 MPa at 2×10^6 cycles, while for single shear riveted joints, a design S–N curve with a slope, $m = 5$ and a fatigue strength of 71 MPa at 2×10^6 cycles should be used. Only few data points from Portuguese riveted bridges fall below these design S–N curves. This result may be justified by the high damage levels experienced by the riveted joints, due to the long bridge operation time. A higher slope, m , of the S–N curve ($\Delta\sigma^m N_f = C$) is suggested by the experimental data, when a comparison is made with the detail 71 from EC3–1-9 [16].

Fatigue design curves can be proposed for single and double shear riveted connections from old Portuguese bridges through the statistical methodologies that were implemented. Concerning the use of ASTM E379 [21], fatigue design curves were defined for $\alpha = -2$ while for Castillo and Fernández-Canteli model [22] the design fatigue curve was computed for the percentile curve corresponding to probability of failure of 5%.

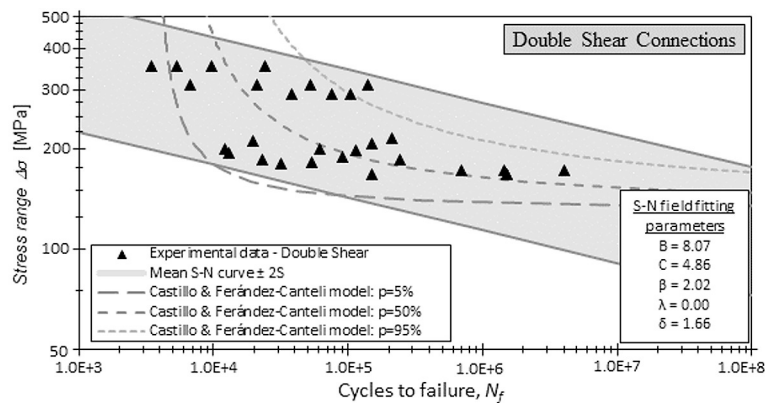


Fig. 20. - S–N fatigue data from **double shear riveted connections** from Portuguese old bridges: statistical analysis using linearized boundaries and Castillo & Fernández-Canteli model [22] (p corresponds to probability of failure).

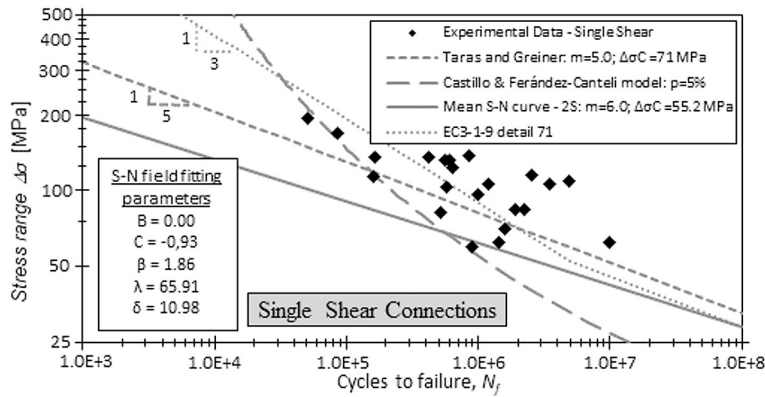


Fig. 21. – Comparison between fatigue design curves obtained from the statistical analysis and the recommended fatigue design curves – Single shear riveted connections.

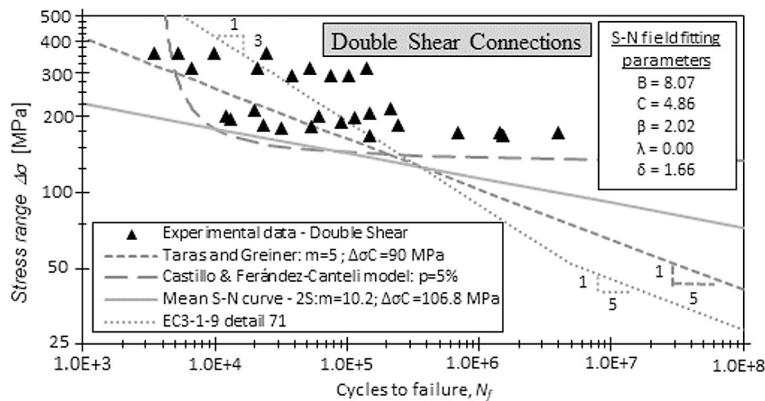


Fig. 22. - Comparison between fatigue design curves obtained from the statistical analysis and the recommended fatigue design curves – Double shear riveted connections.

In Fig. 23 and Fig. 24 are suggested fatigue design curves for single and double shear riveted connections of ancient Portuguese metallic bridges, respectively. For the single shear riveted connections is proposed a design S–N curve with a slope, $m = 5.5$ and a fatigue strength of 58 MPa at 2×10^6 cycles. Whereas, for double shear connections the slope $m = 10$ and the fatigue strength of 110 MPa are suggested to define the design S–N curve. In this way, it is concluded that the proposal presented by Taras and Greiner seems to be consistent with the results of the statistical analysis obtained for the single shear riveted connections. However, based on the statistical analysis of fatigue results of the double shear riveted connections (Eiffel and Fão bridges), it seems not to be consistent. Thus, in this investigation are proposed S–N design curves for single and double cut connections from the old riveted metallic bridges.

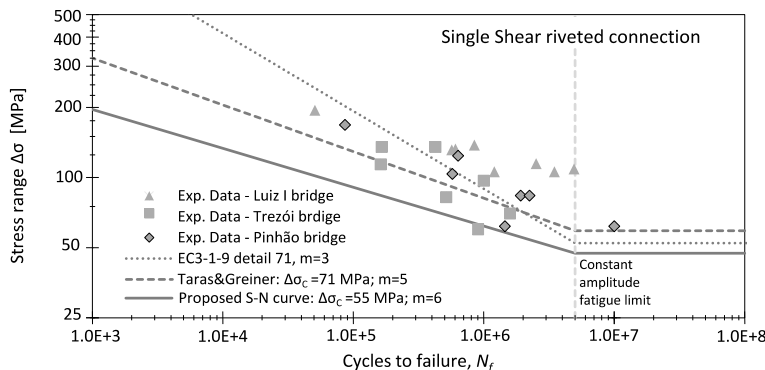


Fig. 23. – Proposed design S–N curves for single shear riveted connections from old Portuguese metallic bridges.

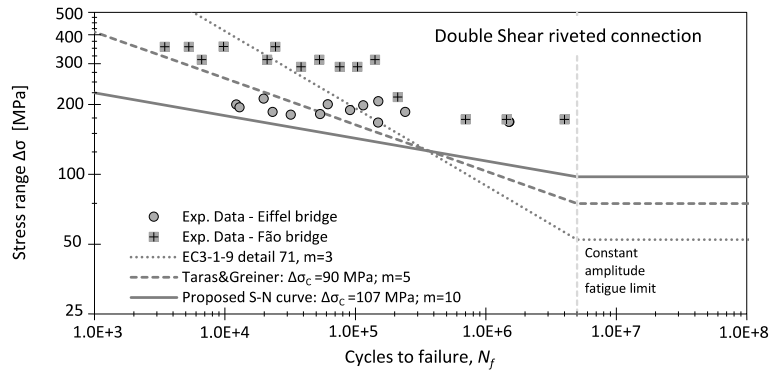


Fig. 24. – Proposed design S–N curves for double shear riveted connections from old Portuguese metallic bridges.

In the case of fatigue design recommendations for double shear riveted connections additional remarks should be stated. It is evident from Fig. 24 that the obtained results from the fatigue tests with specimens extracted from the Eiffel bridge have a significant influence on the proposed curve. Several studies have been performed aiming to characterize the fatigue crack propagation phase of metallic materials from old Portuguese bridges and in particular from the Eiffel bridge [11] [12] [36]. Pereira [36] establish a comparison between longitudinal and transversal fatigue crack propagation properties of Eiffel bridge material through an experimental campaign with CT specimens on both directions. Significantly different values were obtained for Paris law parameters (C and m) in transversal and longitudinal directions as is presented in Table 8. This fact shows that old metallic materials does not present isotropic properties as modern steels.

In Fig. 24 is illustrated the main structural element extracted from the Eiffel bridge in which the double shear riveted specimens were obtained as well as the CT specimens used by Pereira [36] and Correia et al. [11]. It is possible to observe that the fatigue crack obtained with the double shear riveted connections occurred through the transversal directions of the beam and it is interesting to examine that the slope of the proposed S–N curve for this detail is similar to that obtained by Pereira [36]. The differences in the longitudinal and transversal mechanical properties obtained by Pereira [13] suggest that different design approaches should be made depending on the crack propagation direction when old metallic materials are used. Thereby, it is important to mention the need for future investigations on the fatigue resistance of structural details, such as riveted details, in which the crack propagation occur through the longitudinal direction of the beam Fig. 25

In Table 9, a general overview for the different fatigue design approaches of single and double riveted connection is presented.

5. Conclusions

Statistical analysis of S–N fatigue data from original riveted joints was performed in order to propose reliable fatigue design curves and compare them with the recommendations on the standards. This comparison showed that current standards, such as the Eurocode 3, are not able to represent the fatigue behaviour of structural details from old metallic bridges, namely riveted connections. This evidence can be justified by the presence of cracks originated by the prior operation of the bridge or material degradation. It is also worth to underline that in future researches, the problem of microstructural degradation should be considered in fatigue tests. The comparison performed with literature S–N data suggests the need of a riveted joint categorization, in particular the consideration of single and symmetric double shear spllices. Also, slopes m equal to 6 and 10 seem to be more appropriate for single and double shear riveted joints of old metallic bridges, respectively, rather than $m = 3$, as suggested by the current design codes. Finally, it was also noticed that, due to the high level of heterogeneities of old metallic materials, different fatigue behaviours can be found depending on the fatigue crack propagation direction and, thus, different design approaches could be stated. However, more scientific investigations should be performed in order to clarify this aspect.

Table 8

– Paris law parameters (C and m) obtained from CT specimens oriented in transversal and longitudinal directions of the structural element of the Eiffel bridge.

Crack direction	C^*	m^*	R^2
Transversal [36]	6.0E-37	11	0.98
Longitudinal [11]	8.7E-19	5	0.85

* da/dN in mm/cycle and ΔK in $N.mm^{-1.5}$

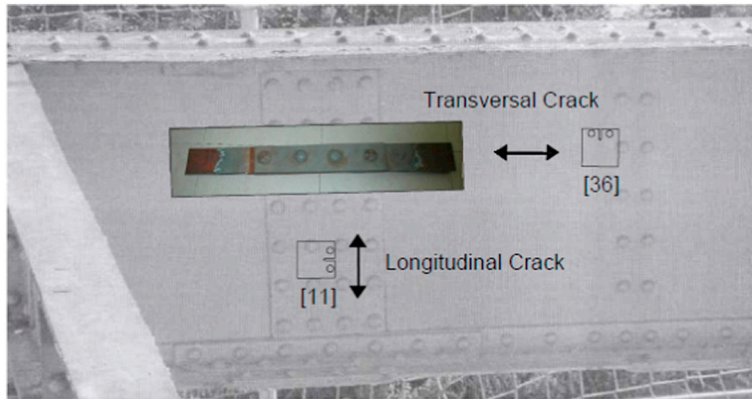


Fig. 25. – Identification of double shear riveted and CT specimens on the structural element which they were extracted.

Table 9

– Summary of fatigue design approaches to single and double riveted connections.

Riveted Single Shear Connections			
Provenience	EC3-1-9 [16]	Taras & Greiner [20]	Proposed design curve by Authors
Design curve	$\Delta\sigma_c = 71 \text{ MPa}$ $m = 3$	$\Delta\sigma_c = 71 \text{ MPa}$ $m = 5$	$\Delta\sigma_c = 55 \text{ MPa}$ $m = 6$
Constructional detail			
Remarks	- $\Delta\sigma$ to be determined on the net cross-section - Riveted details are not included explicitly in EC3-1-9 [16] but this approach is suggested by several authors [19]	- $\Delta\sigma$ to be determined on the net cross-section	- $\Delta\sigma$ to be determined on the net cross-section
Riveted double shear connections			
Provenience	EC3-1-9 [16]	Taras & Greiner [20]	Proposed design curve by Authors
Design curve	$\Delta\sigma_c = 71 \text{ MPa}$ $m = 3$	$\Delta\sigma_c = 90 \text{ MPa}$ $m = 5$	$\Delta\sigma_c = 107 \text{ MPa}$ $m = 10$
Constructional detail			
Remarks	- $\Delta\sigma$ to be determined on the net cross-section - Riveted details are not included explicitly in EC3-1-9 [16] but this approach is suggested by several authors [19]	- $\Delta\sigma$ to be determined on the net cross-section	- $\Delta\sigma$ to be determined on the net cross-section

Acknowledgements

The authors acknowledge the Foundation for Science and Technology (FCT) for the financial support through the doctoral grants SFRH/BD/66497/2009 and SFRH/BD/72434/2010, as well as, the financial support through the post-doctoral grant SFRH/BPD/107825/2015. The authors gratefully acknowledge the funding of ProLife - Prolonging Life Time of Old Steel and Steel-Concrete Bridges (RFSR-CT-2015-00025) by Research Fund for Coal and Steel (RFCs).

References

- [1] B. Akesson, Fatigue Life of Riveted Railway Bridges. PhD Thesis, Chalmers University of Technology, Sweden, 1994.
- [2] R. Crocetti, On some Fatigue Problems Related to Steel Bridges. PhD Thesis, Chalmers University of Technology, Sweden, 2001.
- [3] A.E. Mohammad, Fatigue in Riveted Railway Bridges. PhD Thesis, Chalmers University of Technology, Sweden, 2002.
- [4] G. Lesiuk, M. Szata, M. Bocian, The mechanical properties and the microstructural degradation effect in an old low carbon steels after 100-years operating time, *Arch. Civ. Mech. Eng.* 15 (4) (2015) 786–797.
- [5] G. Lesiuk, M. Szata, Aspects of structural degradation in steels of old bridges by means of fatigue crack propagation, *Mater. Sci.* 47 (1) (2011).
- [6] G. Lesiuk, P. Kucharski, J. Correia, A. De Jesus, C. Rebelo, L. Simões Da Silva, Mixed mode (I+ II) fatigue crack growth of long term operating bridge steel, *Procedia Eng.* 160 (2016) 262–269.
- [7] G. Lesiuk, M. Szata, J. Correia, A. De Jesus, F. Berto, Kinetics of fatigue crack growth and crack closure effect in long term operating steel manufactured at the turn of the 19th and 20th centuries, *Eng. Fract. Mech.*, no. 185 (2017) 160–174.
- [8] Rabięga J, Pękalski G. Material Studies of Pomorski Bridges at the Odra River in Wrocław Town: South, Central and North. Report of the Series SPR 9/2007, I-19, PWR, Wrocław, 2007.
- [9] C. Cremona, et al., Improved Assessment Methods for Static and Fatigue. *Sustain. Dev. Glob. Chang. Ecosyst. Integr. Proj.* (2007) 1–218.
- [10] P. Raposo, et al., Mechanical characterization of ancient portuguese riveted bridges steels, *Eng. Struct. Technol.* 9 (4) (2017) 169–180.
- [11] A. De Jesus, et al., Strain-Life and Crack Propagation Fatigue Data from several Portuguese Old Metallic Riveted Bridges, *Eng. Fail. Anal.* 18 (I) (2011) 148–163.
- [12] J. Correia, et al., Statistical Analysis of Fatigue Crack Propagation Data of Materials from Ancient Portuguese Metallic Bridges, *Frat. ed Integrita Strutt.* (42) (2017) 136–146.
- [13] O. Student, et al., Features of the microstructural and mechanical degradation of long term operated mild steel, *Int. J. Struct. Integr.* 9 (3) (2018) in press.
- [14] J. Kafie-Martinez, et al., Stress Distributions and Crack Formation in Riveted Lap Joints Fastening Thick Steel Plates, *Eng. Fail. Anal.* 91 (2018) 370–381.
- [15] Correia J. An Integral Probabilistic Approach for, Fatigue Lifetime Prediction of Mechanical and Structural Components. PhD Thesis. Faculty of Engineering of the University of Porto, Porto, (2014).
- [16] CEN-TC 250. EN 1993-1-9: Eurocode 3, Design of steel structures – Part 1-9: Fatigue, *Eur. Comm. Stand. Brussels* (2005) 1–34.
- [17] J. Correia, et al., Fatigue behaviour of single and double shear connections with resin-injected preloaded bolts. *IABSE Congr. Stock. 2016 challenges Des. Constr. An Innov. Sustain. Built Environ.* (September, 2016) 327–339.
- [18] A. De Jesus, et al., Fatigue Assessment of Old Riveted Metallic Bridges. In 1st International Conference of the, *International Journal of Structural Integrity* (2012) 25–28, <https://doi.org/10.13140/RG.2.1.3740.5846>.
- [19] J. Di Battista, et al., Fatigue Strength of Riveted Connections, *J. Struct. Eng.* 124 (7) (1998) 792–797.
- [20] A. Taras, Greiner R. Statistical, Background to the Proposed Fatigue Class Catalogue for Riveted Components. Report: Contribution to WG6.1 – Assessment of Existing Steel Structure ECCS TC6, Spring Meeting – Lausanne – March 22–23, (2010).
- [21] A.S.T.M. E739-91, Standard Practice for Statistical Analysis of Linear or Linearized Stress-Life (S-N) and Strain-Life (ε-N) Fatigue Data 1, *Annu. B. ASTM Stand.* (1991) 597–603.
- [22] E. Castillo, Fernández-Canteli a. A Unified Statistical Methodology for Modeling Fatigue Damage, (2009).
- [23] P. Gallegos Mayorga, et al., Design S-N curves for old Portuguese and French riveted bridges connections based on statistical analyses, *Procedia Engineering* (2016) 77–84.
- [24] L. Gallegos Mayorga, et al., Statistical evaluation of fatigue strength of double shear riveted connections and crack growth rates of materials from old bridges, 185 (2017).
- [25] J. Schijve, *Fatigue of Structures and Materials* (New York), (2004).
- [26] J. Schijve, Statistical distribution functions and fatigue of structures, *Int. J. Fatigue* 27 (9) (2005) 1031–1039.
- [27] R. Sanches, A. De Jesus, J. Correia, A. Da Silva, A. Fernandes, A probabilistic fatigue approach for riveted joints using Monte Carlo simulation, *J. Constr. Steel Res.* 110 (2015).
- [28] F. Bastenaire, New method for the statistical evaluation of constant stress amplitude fatigue test results. *Probabilistic Aspect of Fatigue, Am. Soc. Test. Mater. ASTM STP 511* (1972) 9–28.
- [29] J. Spindel, E. Haibach, Some considerations in the statistical determination of the shape of S-N curves, *ASTM STP 744* (1981).
- [30] F. Pascual, W. Meeker, Estimating fatigue curves with the random fatigue-limit model, *Technometrics* 41 (4) (1999) 277–900.
- [31] A. Fernandes, P. De Castro, M. Figueiredo, F. Oliveira, Structural Integrity Evaluation of Highway Riveted Bridges, in: E. In Watanabe, et al. (Ed.), *Bridge Maintenance, Safety and Management (IABMAS'04); Proc. Intern. Conf., Kyoto, 2004*, pp. 839–841.
- [32] M. Figueiredo, et al., Avaliação da integridade estrutural da Ponte do Pinhão DEMEGI/FEUP, (2004).
- [33] T. Silva, A. Fernandes, Ponte Trezói-Estudo do comportamento à fadiga de ligações rebitadas em pontes metálicas antigas. FEUP/DEMEGI. Relatório Proj. fim curso, (2006).
- [34] J. Correia, Development of procedures for fatigue life prediction of riveted connections (in Portuguese), Master Thesis. University of Trás-os-Montes and Alto Douro, Portugal, 2008.
- [35] A. De Jesus, A. Fernandes, A.L.L. Da Silva, J. Correia, Retrofitting of Old Riveted Portuguese Bridges. Past and Current Remnant Life Assessment Research, *ICEM15 – 15th International Conference on Experimental Mechanics Porto – Portugal*, 2012.
- [36] L. Pereira, Assessment of mixed mode fatigue crack propagation in puddled iron from the Eiffel bridge (In Portuguese). MSc Thesis, Faculty of Engineering of the University of Porto, Porto, 2018.